NJC

Accepted Manuscript

This is an *Accepted Manuscript*, which has been through the Royal Society of Chemistry peer review process and has been accepted for publication.

Accepted Manuscripts are published online shortly after acceptance, before technical editing, formatting and proof reading. Using this free service, authors can make their results available to the community, in citable form, before we publish the edited article. We will replace this *Accepted Manuscript* with the edited and formatted *Advance Article* as soon as it is available.

You can find more information about *Accepted Manuscripts* in the Information for Authors.

Please note that technical editing may introduce minor changes to the text and/or graphics, which may alter content. The journal's standard Terms & Conditions and the Ethical guidelines still apply. In no event shall the Royal Society of Chemistry be held responsible for any errors or omissions in this *Accepted Manuscript* or any consequences arising from the use of any information it contains.

ROYAL SOCIETY OF CHEMISTRY

www.rsc.org/njc

Blue-green emitting iridium phenylpyridine complexes using *N*, *N'*-heteroaromatic ancillary ligands

Xu Huixia,*[ab] Sun Peng, [ab] Zhao Dan, [ab] Yang Tingting, [ab] Hao Yuying , [ac] Wang Hua ,[ab] Shi Heping, [d] Xu Bingshe [ab]

[a] *Key Laboratory of Interface Science and Engineering in Advanced Materials, Ministry of Education, Taiyuan University of Technology; Taiyuan 030024; P.R.China*

[b] *Shanxi Research Center of Advanced Materials Science and Technology; Taiyuan 030024; P.R.China;*

[c] *Department of Physics and Optoelectronics, Taiyuan University of Technology; Taiyuan 030024; P.R.China*

[d] *School of Chemistry and Chemical Engineering Shanxi University, Taiyuan 03006, P.R. China*

Abstract: Four Iridium complexes containing different ancillary ligands [Htfmpptz= 2-(5-(4-(trifluoromethyl)phenyl)-2H-1,2,4-triazol-3-yl)pyridine, Hfpptz= 2-(5-(4-fluorophenyl)-2H-1,2,4-triazol-3-yl)pyridine and Htfmptz= 2-(5-(trifluoromethyl) -2H-1,2,4-triazol-3-yl)pyridine) and ppy (2-phenylpyridine) as main ligand were synthesized and characterized. Their molecular structures were identified by X-ray single crystal diffraction. The effects of ancillary ligands on the photophysical and luminescent behavior were investigated. The emission maximum peaks of $(ppy)_2Ir(tfmpptz)$, $(ppy)_2Ir(fpptz)$ and $(ppy)_2Ir(tfmptz)$ in CH_2Cl_2 solution appear at 485, 487 and 483 nm, respectively. Phosphorescent organic light-emitting devices (PhOLEDs) were fabricated using these complexes doped in CBP as emitting layer.

1. Introduction

Phosphorescent organic light-emitting devices (PhOLEDs) have attracted huge interests due to high quantum efficiency by utilizing both singlet and triplet excitons [1-3]. Ir(III) complexes, acting as emitters in PhOLEDs, have the better performances among numerous metal

complexes so far [4-6]. The homoleptic (Ir(*C*^*N*)$_3$) and heteropleptic (Ir(*C*^*N*)$_2$(LX)), in which *C*^*N* is a cyclometalated ligand and LX is an ancillary ligand, have been developed [7-8]. Since the field strength of ancillary ligand controls Ir-centered d-(t_{2g}) orbital energy, the singlet metal-to-ligand charge transition (^{1}MLCT) state energy can be tuned by introducing various ancillary ligands without altering the cyclometalate ligand-centered (LC) transition states [9]. And in turn, the emission spectra of Ir(*C*^*N*)$_2$(LX) complexes are changed [10, 11]. However, choosing appropriate ancillary ligand to realize blue-light emission still remains an important challenge. It has been demonstrated that the ancillary ligand of *N*, *N*'-heteroaromatic (*N*^*N*) has higher triplet energy level and lone electron pair of N atom can regulate effectively the lowest unoccupied molecular orbital (LUMO) levels[12-15]. These complexes with *N*^*N* ligands prefer to emitting the blue and green-blue light [16-18].

It is well known that tris(2-phenylpyridine)iridium (Ir(ppy)$_3$) is the best green-light emitting materials and has excellent electron injection and transport characteristics. In this paper, we will report the blue-green-emitting complexes by introducing the *N*^*N* ligands of 2-(5-(4-(trifluoromethyl)phenyl)-2H-1,2,4-triazol-3-yl)pyridine (Htfmpptz), 2-(5-(4-fluorophenyl)-2H-1,2,4-triazol-3-yl)pyridine (Hfpptz) and 2-(5-(trifluoromethyl) -2H-1,2,4-triazol-3-yl)pyridine (Htfmptz) as ancillary ligand into Ir(ppy)$_3$. The molecular structures of all four complexes are described in Scheme 1.

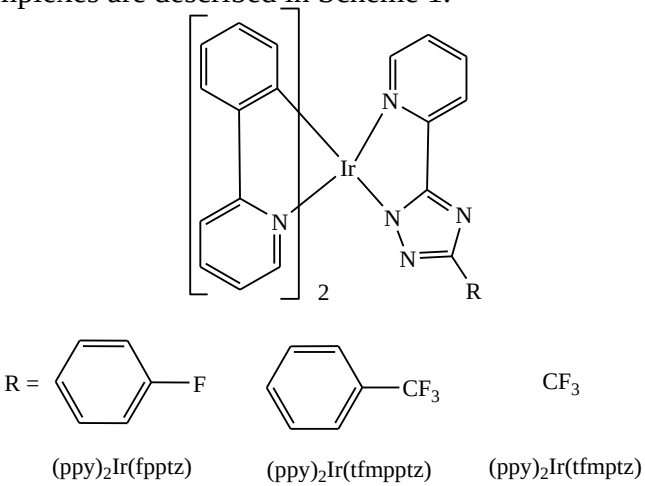

(ppy)$_2$Ir(fpptz) (ppy)$_2$Ir(tfmpptz) (ppy)$_2$Ir(tfmptz)

Scheme 1. Molecular structures of (ppy)$_2$Ir(fpptz), (ppy)$_2$Ir(tfmpptz) and (ppy)$_2$Ir(tfmptz)

2. Experimental Section

2.1 General Information

X-ray single-crystal diffractions of all complexes were performed on Bruker SMART APEX II diffractometer with Mo Ka radiation (λ=0.710 73 Å). The structures were solved with direct methods (SHELX-97) and refined with full-matrix least-squares technique. All non-hydrogen atoms were refined anistropically and hydrogen atoms of organic ligands were geometrically placed.

All calculations were performed using Gaussian 03 package by employing experimental parameters determined by X-ray single-crystal diffraction as input file. The geometry optimization of ground state by density functional theory (DFT) were carried out using B3LYP functional with 6-31G(d) basis sets [19, 20], except for LANL2DZ basis sets for Ir atom.

^{1}H NMR data were recorded with Bruker 600 MHz spectrometers. FT-IR spectra were measured with a Nicolet 7199B spectrometer in KBr pellets in the range of 4000-400 cm^{-1}. Elemental analyses of carbon, hydrogen, and nitrogen were performed on a Vario EL microanalyzer. UV-vis absorption spectra were recorded by Lambda Bio 40. The fluorescence spectra were examined by HORIBA FluouoMax-4 spectrophotometer in dichloromethane (CH_2Cl_2) solution. The absolute florescence quantum yields of solution (2×10^{-5} mol/L) were measured by a HORIBA FluouoMax-4 equipped with an integrating sphere. Cyclic voltammetry was performed with Autolab/PG STAT302 in a one-compartment electrolysis cell using two platinum wires as working electrode and counter, a calomel electrode as reference. $TBAPF_6$ was used as supporting electrolyte (0.1 M). Cyclic voltammetric behaviors were monitored at scan rate 50 mV/s.

Organic layers were fabricated by high-vacuum (3×10^{-4} Pa) thermal evaporation onto a glass substrate precoated with an ITO (indium tin oxide) layer. The device structures were ITO / NPB (40 nm)/ CBP: $(ppy)_2Ir(N\text{^}N)$ (6 wt%, 30 nm)/ TPBi (35 nm)/ LiF(1 nm)/ Al (200

nm). Materials used for the device are NPB (*N*, *N*'-Bis (naphthalen)-*N*, *N*'-bis (phenyl)-benzidine) for hole-transport layer, Ir(III) complexes (6 wt%) in CBP (4,4'-*N*,*N*'-dicarbazolebiphenyl) for emitting layer, TPBi (2, 2′,2″-(1, 3, 5-phenylene) tris (1-phenyl-1H-benzimidazole) for electron-transport layer. The electroluminescent (EL) spectra were measured by PR-655 spectrofluorometer. The luminance - voltage - current density (V-*L*-*J*) and current efficiency - current density - power efficiency (η_c-*J*-η_p) characteristics of PhOLEDs were recorded on Keithley 2400 Source Meter and L-2188 spot Brightness Meter.

2.2 Synthesis of complexes

Solvents for chemical synthesis were purified according to the standard procedures. All reactions were carried out under a dry and oxygen-free atmosphere. The *N*^*N* ligands of Htfmpptz, Hfpptz and Htfmptz were synthesized according to the Ref.15. 2-Phenylpyridine (H ppy) and Iridium trichloride hydrate in 2-ethoxyethanol and water (3:1) solution were treated to obtain the chloride-bridged dimer [{$(ppy)_2Ir(\mu\text{-}Cl)\}_2$] according to the literature procedure [21].

Complex $(ppy)_2Ir(tfmpptz)$: {$(ppy)_2Ir(\mu\text{-}Cl)\}_2$, K_2CO_3 and the Htfmpptz ligands (2:1:20) were added in 2-ethoxyethanol (25 ml) at 140℃ for 24 h . After cooling to room temperature, the mixture was poured into water for extraction. The residue was dried in vacuum for 12 h and then recrystallized from methanol/acetonitrile/dichloromethane (1:3:30) to obtain the complexes $(ppy)_2Ir(tfmpptz)$ in a yield of 65%. ^{1}H NMR (600 MHz, DMSO-d_6): δ 8.22 (1H, s), 8.20 (1H, s), 8.19 (1H, d), 8.15 (1H, s), 8.14 (1H, s), 8.06 (1H dt), 7.89-7.82 (3H, m), 7.83 (1H, d), 7.71 (1H, s), 7.70 (1H,s), 7.65 (2H, dd), 7.62 (1H, d), 7.40 (1H, ddd), 7.20 (1H, ddd), 7.15 (1H, ddd), 6.97 (1H, dt), 6.90 (1H, dt), 6.88 (1H,dt), 6.78 (2H, dt). FT-IR (KBr) cm^{-1}: 2025, 1644, 1611, 1478, 1420, 1324, 1167, 1121, 1063, 868, 764, 727, 503. Anal. calcd for

$C_{36}H_{24}F_3IrN_6$, C, 54.74; H, 3.06; N, 10.64; found: C, 54.81; H, 3.40; N, 10.64.

Complex $(ppy)_2Ir(fpptz)$: This complex was prepared according to the procedure for the synthesis of $(ppy)_2Ir(tfmpptz)$, in a yield of 70 %. ^1H NMR (600 MHz, DMSO-d_6): δ 8.19-8.15 (3H, m), 8.02 (1H, t), 7.95 (2H, dd), 7.86-7.83 (3H, m), 7.80 (1H, d), 7.64 (1H d), 7.60 (2H, d), 7.35 (1H, t), 7.19-7.12 (4H, m), 6.95 (1H, t), 6.88 (1H, t), 6.85 (1H, t), 6.75 (1H, t), 6.19 (2H, dd). FT-IR (KBr) cm^{-1}: 2029, 1640, 1606, 1586, 1515, 1482, 1424, 1221, 1154, 760, 628. $C_{35}H_{24}FIrN_6$, C, 56.82; H, 3.27; N, 11.36; found: C, 56.90 H, 3.18; N, 11.38.

complex $(ppy)_2Ir(tfmptz)$: This complex was prepared according to the procedure for the synthesis of $(ppy)_2Ir(tfmpptz)$, in a yield of 60 % ^1H NMR (600 MHz, DMSO-d_6): δ 8.21-8.17 (3H, m), 8.07 (1H, dt), 7.89-7.84 (3H, m), 7.93 (1H, d), 7.64 (1H, d), 7.58 (1H d), 7.51 (1H, d), 7.45 (1H, dt), 7.21 (1H, dt), 7.13 (1H, dt), 6.96 (1H, dt), 6.89-6.84 (2H, m),6.74 (1H, dt), 6.19 (1H, d), 6.14 (1H, dt), 6.93 (1H, s), 6.88 (1H, dt), 6.86 (1H, dt), 6.61 (1H, s), 6.33 (2H, t), 6.01 (1H, d). FT-IR (KBr) cm^{-1}: 2029, 1635, 1606, 1478, 1204, 1134, 760, 574. $C_{30}H_{20}F_3IrN_6$, C, 50.84; H, 2.82; N, 11.77; found: C, 51.02 H, 3.20; N, 11.67.

3. Results and Discussion

3.1 Single-crystal structures

The X-ray single-crystal structure diffraction studies were carried out to reveal the exact structures of $(ppy)_2Ir(tfmpptz)$, $(ppy)_2Ir(fpptz)$ and $(ppy)_2Ir(tfmptz)$. The crystal structure data are shown in Table 1. These complexes show distorted octahedral geometries with two cyclometalated ppy ligand and one *N^N* ligand surrounding the iridium metal center, as displayed in Fig. 1. It is obvious that ppy ligands in complexes $(ppy)_2Ir(tfmpptz)$ and $(ppy)_2Ir(fpptz)$ are located in the trans orientation, showing the typical coordinated geometries [22]. The coordination pattern for ppy chelates in $(ppy)_2Ir(tfmptz)$ are changed into cis orientation in Fig. 1c. The associated Ir-N distances on the *N^N* ligands are significantly shorter than that of ppy ligands because of the stronger electron-withdrawing abilities of

triazol. The Ir-N bond lengths between Ir(III) metal and tfmptz for $(ppy)_2$(tfmptz) (Ir-N5=2.031 Å, Ir-N6=2.033 Å) are shorter than that of $(ppy)_2$Ir(fpptz) (Ir-N5=2.054 Å, Ir-N6=2.038 Å) and $(ppy)_2$Ir(tfmpptz) (Ir-N5=2.032 Å, Ir-N6=2.042 Å) due to the isomerization of two ppy chelates. The phenyl-triazole torsional angle of N3-C7-C8-C13 in $(ppy)_2$Ir(tfmpptz) is closer to coplanarity (4.4 °). While, the phenyl ring twists to the opposite position with respect to the triazole ring with the value of -26.8 °.

Table 1 Crystallographic data for $(ppy)_2$Ir(fpptz), $(ppy)_2$Ir(tfmpptz) and $(ppy)_2$Ir(tfmptz)

	$(ppy)_2$Ir(fpptz)	$(ppy)_2$Ir(tfmpptz)	$(ppy)_2$Ir(tfmptz)
Empirical formula	$C_{35}H_{24}FIrN_6$	$C_{36}H_{24}F_3IrN_6$	$C_{30}H_{20}F_3IrN_6$
Crystal size, (mm^3)	0.23×0.21×0.19	0.19×0.14×0.09	0.23×0.21×0.19
Formula weight	739.80	789.81	713.72
Temperature, K	296(2)	293(2)	293(2)
Wavelength, (Å)	0.71073	0.71073	0.71073
Crystal system	Orthorhombic	Triclinic	Triclinic
Space group	*Pbca*	*P*-1	*P*-1
a, (Å)	13.163(7)	9.979(5)	9.307(7)
b, (Å)	20.032(11)	12.906(7)	12.792(9)
c, (Å)	23.737(13)	13.397(7)	13.798
α (deg)	90	94.040(5)	96.684(7) °
β (deg)	90	94.595(5) °	98.707(7) °
γ (deg)	90	105.072(5) °	109.386(6) °
Volume ($Å^3$)	6259(6)	1653.2(15)	1507.1(19)
Z	8	2	2
Reflections collected	35723 / 5632 [R(int) = 0.0906]	11818 / 5861 [R(int) = 0.0486]	10862 / 5526 [R(int) = 0.0406]
Goodness-of-fit on F^2	1.002	1.009	1.026
R indices (all data)	R_1 = 0.0780, wR_2 = 0.0791	R_1= 0.0543, wR_2= 0.0815	R_1 = 0.0568, wR_2 = 0.0900

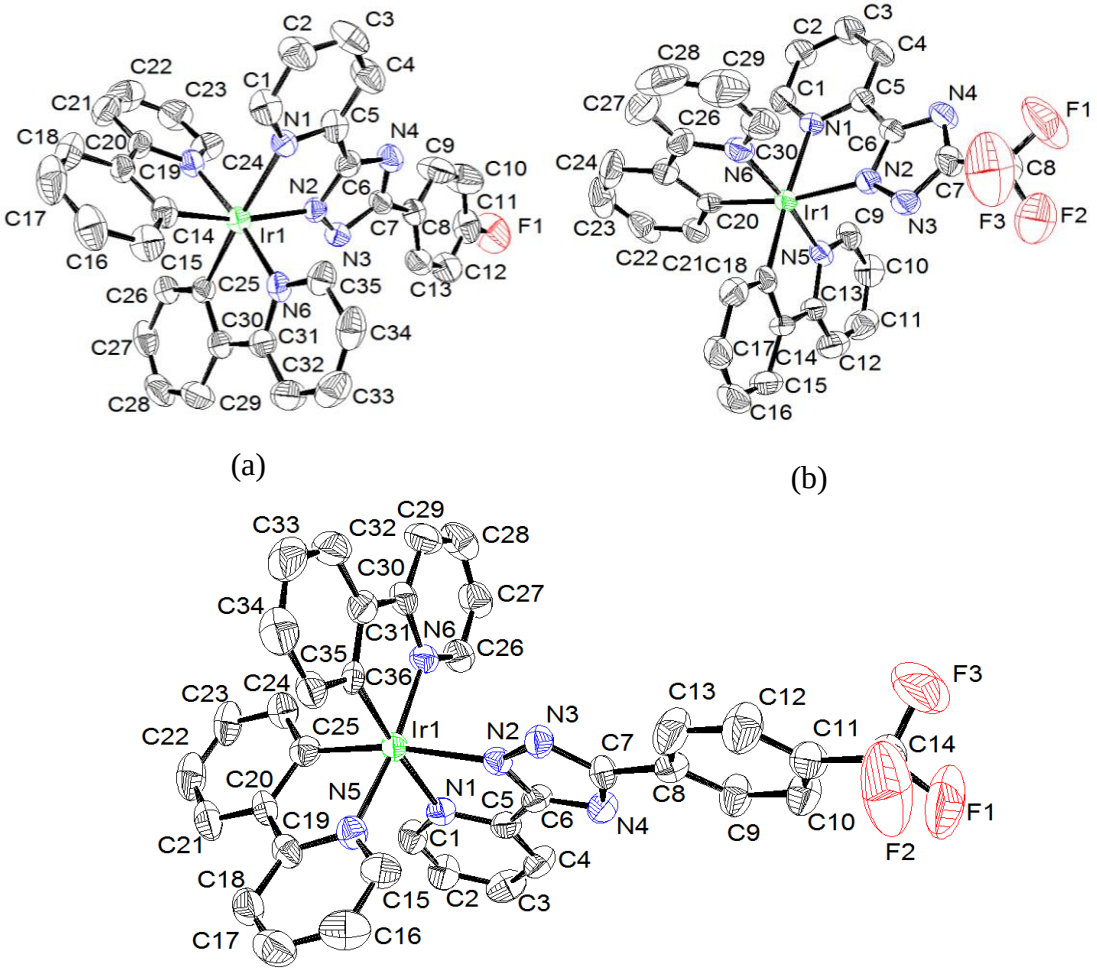

Fig.1. ORTEP diagrams of $(ppy)_2Ir(fpptz)$ (a), $(ppy)_2Ir(tfmpptz)$ (b) and $(ppy)_2(tfmptz)$ (c) with thermal ellipsoid show at 30% probability level. (Selected bond distances and angles for $(ppy)_2Ir(fpptz)$: Ir(1)-N(1)=2.182(5), Ir(1)-N(2)=2.133(5), Ir(1)-N(5)=2.054(5), Ir(1)-N(6)=2.038(5), Ir(1)-C(14)=1.999(6), Ir(1)-C(25)=2.009(6)Å; N(2)-Ir(1)-N(1)=76.25(19), N(5)-Ir(1)-N(1)=88.89(19), C(14)-Ir(1)-C(25)=89.2(2), C(14)-Ir(1)-N(5)=80.2(2)°. Selected bond distances and angles of $(ppy)_2Ir(tfmpptz)$: Ir(1)-N(1)=2.175(5), Ir(1)-N(2)=2.124(5), Ir(1)-N(5)=2.032(5), Ir(1)-N(6)=2.042(5)Å, Ir(1)-C(15)=2.003(6), Ir(1)-C(26)=2.013(6); N(2)-Ir(1)-N(1)=76.48(19), N(5)-Ir(1)-N(1)=89.8(2), C(15)-Ir(1)-C(26)=89.9(2), C(15)-Ir(1)-N(5)=80.1(2)°; Selected bond distances and angles of $(ppy)_2(tfmptz)$: Ir(1)-N(1)=2.165(5), Ir(1)-N(2)=2.126(5), Ir(1)-N(5)=2.031(6), Ir(1)-N(6)=2.033(6), Ir(1)-C(19)=2.024(7), Ir(1)-C(30)=2.011(7)Å; N(2)-Ir(1)-N(1)=76.4(2), N(5)-Ir(1)-N(2)=92.1(2), C(19)-Ir(1)-C(30)=87.6(2), N(5)-Ir(1)-N(2)=92.1(2)°)

3.2 Absorption and emission spectra

Fig.2 shows the UV-vis absorption spectra of complexes $(ppy)_2Ir(tfmpptz)$, $(ppy)_2Ir(fpptz)$ and $(ppy)_2Ir(tfmptz)$ in CH_2Cl_2 solution. The time-dependent DFT (TD-DFT) calculations indicated that the intense absorption bands at 250-270 nm are mainly attributed to the π-π* transition of the triazole ligands and the shoulders at 280-320 nm are due to the transitions centered on the ppy ligand. The weaker absorption bands around 350-360 nm are origin from the spin-allowed singlet-to-singlet metal-to-ligand charge-transfer (^{1}MLCT). The absorption bands of >400 nm, which were amplified and displayed in insert, are assigned to mixtures of spin-forbidden singlet-to-triplet ^{3}MLCT and ^{3}LC known for iridium complexes because of the strong spin-orbit coupling [23]. The absorption of complex $(ppy)_2Ir(fpptz)$ with the lager phenyl-triazole torsional angle has a littler blue shift relative to $(ppy)_2Ir(tfmpptz)$.

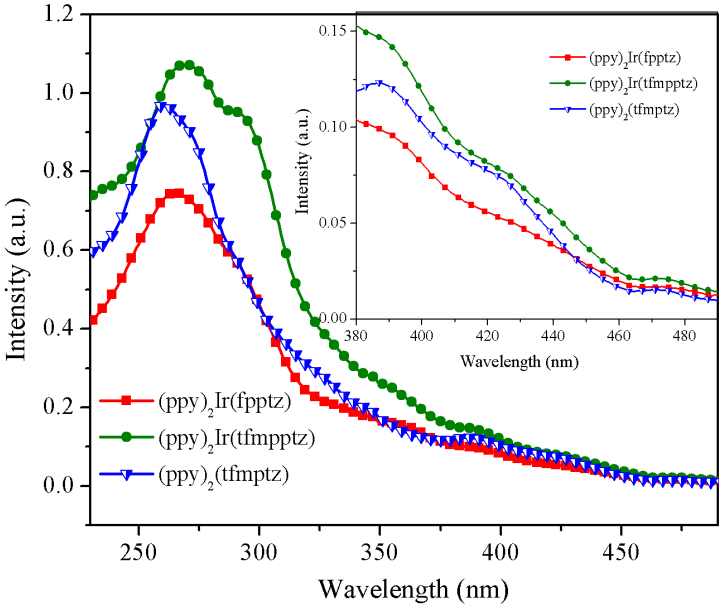

Fig.2 The absorption spectra of complexes $(ppy)_2Ir(fpptz)$, $(ppy)_2Ir(tfmpptz)$ and $(ppy)_2Ir(tfmptz)$ in CH_2Cl_2 solution. The T_1 absorption transitions are shown in the inset.

The optical energy gaps (E_g) of the complexes was calculated according to their absorption edges and listed in Table 2. The E_g of $(ppy)_2Ir(tfmpptz)$, $(ppy)_2Ir(fpptz)$ and

$(ppy)_2Ir(tfmptz)$ are 2.61, 2.60 and 2.62 eV, which are larger than that of $Ir(ppy)_3$ [8]. The complex of $(ppy)_2Ir(tfmpptz)$ and $(ppy)_2Ir(fpptz)$ show the smaller E_g than $(ppy)_2Ir(tfmptz)$, which are due to the increased the conjugation.

The titled complexes exhibit the bright blue-green emission at room temperature in CH_2Cl_2 solution and the emission spectrum of $Ir(ppy)_3$ was also measured under the same conditions, as shown in Fig.3. The emission spectra of complexes $(ppy)_2Ir(N^\wedge N)$ have the similar profiles with the intense peaks at around 485 nm and a shoulder near 513 nm. The vibronic structure of the emission bands indicates a large amount of ^{3}LC character. The peaks of around 485 nm may be origin from the N^N ligands. Meanwhile, the emission shoulder at 513 nm are consistent with the maximum emission peak of $Ir(ppy)_3$, which are due to the ^{3}MLCT and ^{3}LC states centered on the ppy ligands [24]. The order of the maximum peaks at emission spectra is $(ppy)_2Ir(tfmptz) < (ppy)_2Ir(tfmpptz) < (ppy)_2Ir(fpptz) < Ir(ppy)_3$. This emission behavior was attributed to the increasing electron-withdrawing abilities of the ligands along to the same order [15]. The poor overlap between the emission and absorption bands are due to the origin of emission possessing excessive ligand-centered ππ* and relatively low MLCT character.

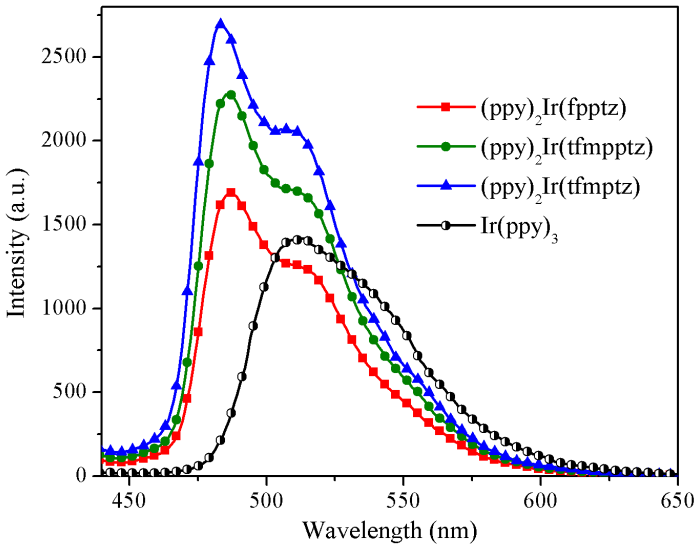

Fig. 3. The emission spectra of complexes ($(ppy)_2Ir(N^\wedge N)$) and $Ir(ppy)_3$ in CH_2Cl_2 solution at room temperature

The photoluminescent quantum yields (PLQY) of $(ppy)_2Ir(tfmpptz)$, $(ppy)_2Ir(tfmptz)$ and $(ppy)_2Ir(fpptz)$ are 60, 47 and 44%, respectively. The complex of $(ppy)_2Ir(tfmpptz)$ has a higher quantum yields (Φ) than others because of the better coplanarity and the increased conjugation.

3.3 Electrochemical properties

The electrochemical behaviors of all complexes were examined by cyclic voltammetry and the values of E_{HOMO} (HOMO: the highest occupied molecular orbital) and E_{LUMO} (E_{LUMO}were obtained according to the equation of ($E_{LUMO} = E_g - E_{HOMO}$) are also listed in Table 2. The HOMO/LUMO levels of $(ppy)_2Ir(tfmpptz)$ and $(ppy)_2Ir(fpptz)$ are -5.64/-3.03 and -5.78/-3.20 eV. It is noticeable that the introduction of ancillary ligand can be make the HOMO and LUMO stabilized relative to $Ir(ppy)_3$ (The HOMO/LUMO levels of $Ir(ppy)_3$ are -2.9/-5.3 eV [26]). These lower LUMO levels benefit the electron injection from the cathode in devices.

Table 2. Absorption and emission data, HOMO, LUMO levels and optical bandgap (E_g) and quantum yields (Φ) in CH_2Cl_2 solution of all titled complexes

Complexes	λ_{abs} (nm)	$\lambda_{max,\ em}$ (nm)	HOMO [a] (eV)	LUMO [b] (eV)	E_g [c] (eV)	Φ (%)
$(ppy)_2Ir(tfmpptz)$	269, 292, 355, 387, 426, 474	485, 513	-5.64	-3.03	2.61	60
$(ppy)_2Ir(fpptz)$	264, 284, 348, 389, 425, 475	487, 516	-5.78	-3.20	2.60	44
$(ppy)_2Ir(tfmptz)$	250, 298, 351, 387, 424, 474	483, 510			2.62	47
$Ir(ppy)_3$		510	-5.3	-2.9	2.4	

[a] $HOMO = eE_{0x} - 4.74$, E_{0x} obtained from the cyclic voltammetry [b] $LUMO = HOMO - E_g$; [c] E_g obtained from the onset of Uv-Vis absorption spectra.

In order to investigate the photophysical properties of the compounds, DFT was applied to molecular orbitals studies. The results indicated that complexes of $(ppy)_2Ir(tfmpptz)$, $(ppy)_2Ir(fpptz)$ and $(ppy)_2Ir(tfmptz)$ have the similar frontier molecular orbitals. Taking the

$(ppy)_2Ir(tfmpptz)$ for example in Fig. 4, the HOMOs are absolutely dominated by the Ir^{3+} cores involving the contributions of the Ir d-orbitals and the π-orbitals attributed to the phenyls of ppy and 1,2,4-triazole, and the LUMOs are largely located at π* orbital from ppy and pyridine of tfmpptz. One of the ppy and 4-(trifluoromethyl)phenyl moieties have no contribution to LUMO and LUMO+1.

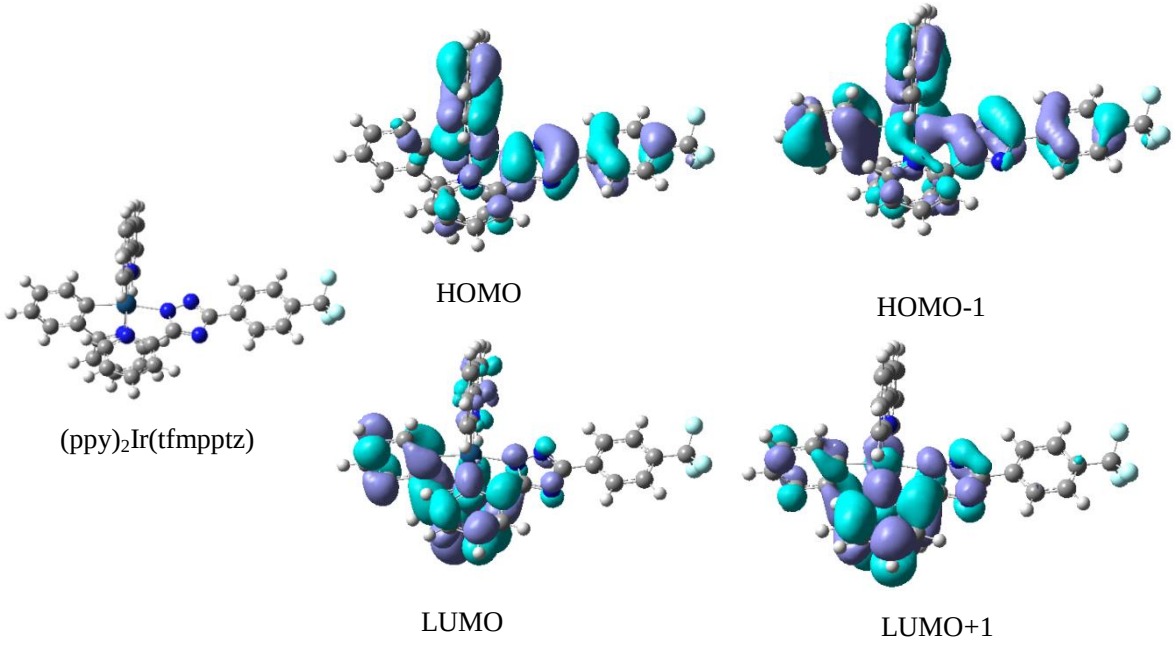

Fig.4. Optimized molecular structures and frontier molecular orbitals characterization of $(ppy)_2Ir(tfmpptz)$

3.4 Electroluminescent Characterization

The electroluminescent properties of the complexes were examined by doping them into the host as emitting layers. The device A-C structures are ITO / NPB (40 nm)/ CBP: $(ppy)_2Ir(N^\wedge N)$ (6 wt%, 30 nm)/ TPBi (35 nm)/ LiF(1 nm)/ Al (200 nm). The complexes $(ppy)_2Ir(N^\wedge N)$ consist of $(ppy)_2Ir(fpptz)$ (device A), $(ppy)_2Ir(tfmpptz)$ (device B), and $(ppy)_2Ir(tfmptz)$ (device C). Normalized EL spectra peaks of devices A - C appear at 490 nm and shoulder peak at about 516-519 nm, as displayed in Fig. 5. The spectral features and emission energies in EL resemble those in PL very closely, indicating that the emission originates from the same species in both EL and PL. The emissions of NPB and CBP was not

observed, suggesting that the complete energy transfer occurs from CBP to complexes $(ppy)_2Ir(N^{\wedge}N)$.

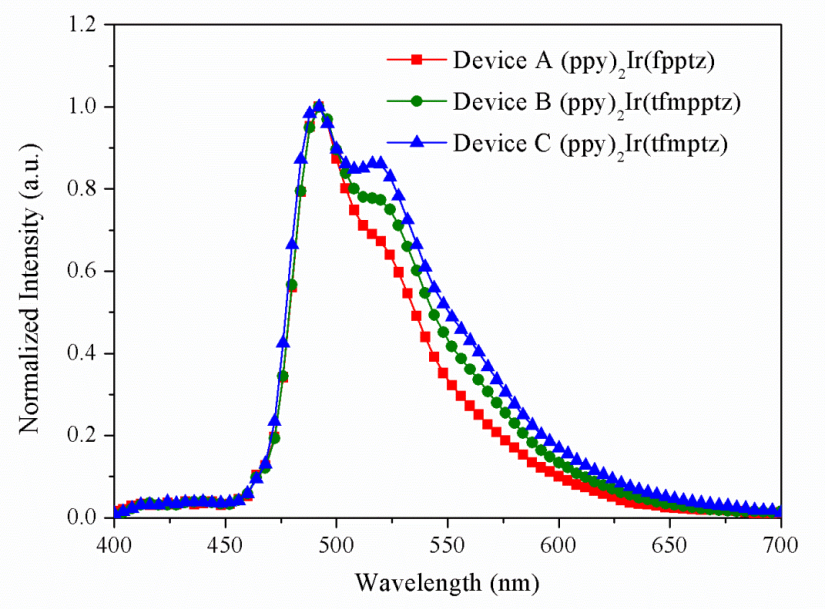

Fig. 5. The EL spectra of device A-C at voltage of 5V

The devices A- C show the maximum luminance (L_{max}) of 7 724 cd/m^2 at voltage of 6 V, 7 261 cd/m^2 at voltage of 5.7 V and 5 114 cd/m^2 at voltage of 5.7 V, respectively, as displayed in Fig. 6a. The lower turn-on voltages (the voltage at a brightness of 1 cd/m^2) were 3.3, 3.2 and 3.0 V. The device A and B have the similar performances based on the $(ppy)_2Ir(fpptz)$ and $(ppy)_2Ir(tfmpptz)$ with the same current and power efficiency (η_c=4.1 cd/A and η_p=3.2 lm/W) in Fig. 6b. The complex $(ppy)_2Ir(tfmptz)$ (device C) exhibit the better performances with higher current efficiency (η_c=4.5 cd/A) and higher power efficiency (η_p=3.7 lm/W). But the device A and B exhibit the lower roll-off in efficiency, which are attributed to the increased conjugation due to the phenyl group of complexes $(ppy)_2Ir(fpptz)$ and $(ppy)_2Ir(tfmpptz)$. Compared with device B, the device A have the lower roll-off in efficiency because the larger the torsional angle between the triazole and phenyl ring results in a larger steric hindrance. Consequently, triplet-triplet annihilation can be weakened.

Table 3. The performances of devices A-C

Device	V_{on} [a] V	L_{max} [b] cd/m^2	η_c [c] cd/A	η_p [d] lm/W	λ_{max} [e] nm
A	3.3	7 724	4.1	3.2	491, 519
B	3.2	7 261	4.1	3.2	490, 518
C	3.0	5 114	4.5	3.7	490, 515

[a] the voltage at a brightness of 1cd/m^2; [b] the maximum luminance; [c] the maximum current efficiency; [d] the maximum power efficiency; [e] the peak of EL spectra

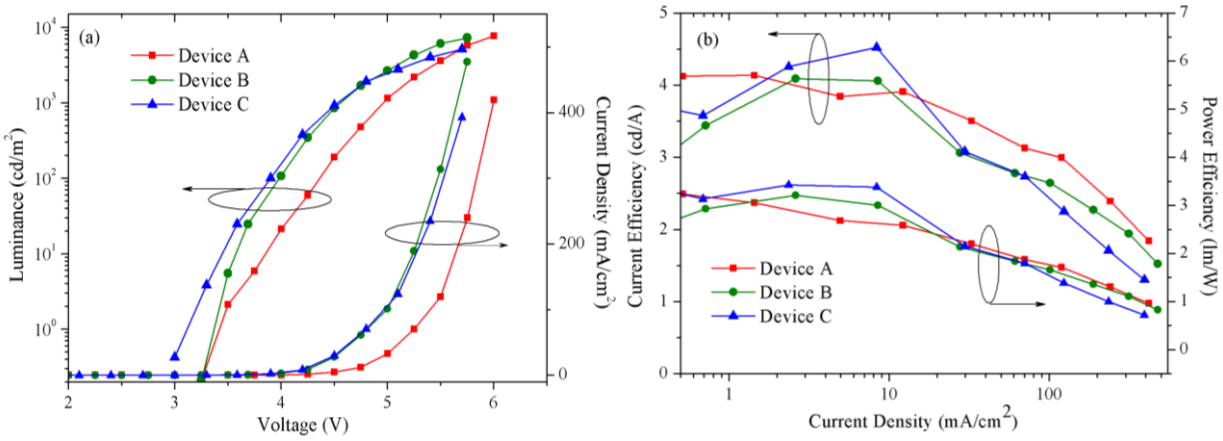

Fig. 6.The L- V- J (a) and η_c-J-η_p (b) curves of devices A-C

4. Conclusions

The molecular structures, photophysical, electrochemical and electroluminescent properties of four (ppy)$_2$Ir(N^N) complexes have been investigated. These complexes exhibit wider optical energy gaps than that of tris (2-phenylpyridine) iridium. Their PL and EL spectra are located in the bluish-green light range. The devices by using (ppy)$_2$Ir(N^N) complexes as guest were fabricated in order to character the electroluminescent properties. The device employing (ppy)$_2$Ir(tfmpptz) doped in CBP as light-emitting layer had a better performance. The relationships between molecular structure and photoelectric performances were discussed in detail.

Acknowledgments

This work was financially supported by International Science & Technology Cooperation Program of China (2012DFR50460); National Natural Scientific Foundation of China (21071108, 60976018, 21101111, 61274056 and 61205179); Natural Science Foundation of Shanxi Province (2011021022-2 and 2010021023-2); Program for Changjiang Scholar and Innovation Research Team in University (IRT0972); Key Scientific and Technological Project of Shanxi Province (20120321019).

*__Corresponding author__.

Xu Huixia Tel: +86-0351-6014852, Fax: +86-0351-6010311

E-mail: xuhuixia@tyut.edu.cn

References

[1] Y. M. Jin, C. C. Wang, L. S. Xue, T. Y. Li, S. Zhang, X. Liu, X. Liang, Y. X. Zheng, J. L. Zuo, *J. Organomet. Chem.*, 2014, **765**, 39-45.

[2] W.-Y. Wong and C.-L. Ho, *J. Mater. Chem.*, 2009, **19**, 4457-4482.

[3] E. Orselli, J. Maunoury, D. Bascour, J. P. Catinat, *Org. Electron.*, 2012, **13**, 1506-1510.

[4] W.-Y. Wong and C.-L. Ho, *Coord. Chem. Rev.*, 2009, 253, 1709-1758.

[5] L. Ying, C.-L. Ho, H. Wu, Y. Cao, W.-Y. Wong, *Adv. Mater*., 2014, **26**, 2459-2473.

[6] X. Yang, G.-J. Zhou, W.-Y. Wong, *J. Mater. Chem.* C, 2014, **2**, 1760-1778.

[7] G. G. Shan, H. B. Li, H. T. Cao, D. X. Zhu, Z .M. Su, Y. Liao，*J. Organomet. Chem.*, 2012, **713**, 20-26.

[8] M. C. Suh, H. Y. Shin, S. J. Cha, *Org. Electron.*, 2013, **14**, 2198-2203.

[9] L. C. Chen, Z. H. Ma, J. Q. Ding, L. X. Wang, X. B. Jing, F. S. Wang, *Org. Electron.*, 2012, **13**, 2160-2166.

[10] S. J. Lee, J. S. Park, M. Song, I. A. Shin, Y. I. Kim, J. W. Lee, J. W. Kang, Y. S. Gal, S.

Kang, J. Y. Lee, S. H. Jung, H. S. Kim, M. Y. Chae, S. H. Jin, *Adv. Funct. Mater.*, 2009, **19**, 2205-2212.

[11] K. Y. Lu, H. H. Chou, C. H. Hsieh, Y. H.Yang, H. R.Tsai, H. Y. Tsai, L. C. Hsu, C. Y. Chen, I. C. Chen, C. H. Cheng, *Adv. Mater.*, 2011, **23**, 4933-4937.

[12] C.-L. Ho and W.-Y. Wong, *New J. Chem*., 2013, **37**, 1665-1680.

[13] G.-J. Zhou, C.-L. Ho, W.-Y. Wong, Q. Wang, D. Ma, L. Wang, Z. Lin, T. B. Marder, A. Beeby, *Adv. Funct. Mater*., 2008, **18**, 499-511.

[14] C.-L. Ho, Q. Wang, C. S. Lam, W.-Y. Wong, D. Ma, L. Wang, Z. Q. Gao, C. H. Chen, K. W. Cheah, Z. Lin *Chem. –Asian J.*, 2009, **4**, 89-103.

[15] H. X. Xu, Y. Yue, L. T. Qu, Y. Y. Hao, H. Wang, L. Q. Chen, B. S. Xu, *Dyes Pigments*, 2013, **99**, 67-73.

[16] X. Zhang, C. Jiang, Y. Mo, Y. Xu, H. Shi, Y. Cao, *Appl. Phys. Lett.*, 2006, **88**, 051116.

[17] F. Dumur, M. Lepeltier, B. Graff, E. Contal, G. Wantz, J. Lalevée, C. R. Mayer, D. Bertin, D. Gigmes, *Synth. Met.*, 2013,**182**, 13-21.

[18] B. Chen, Y. Li, W. Yang, W. Luo, H. Wu, *Org. Electron*., 2011, **12**, 766-773.

[19] A. D. Becke, *Phys. Rev. A*, 1998, **38**, 3098-3100.

[20] C. Lee, W. T. Yang, R. G. Parr, *Phys. Rev. B*, 1988; **37**, 785-789.

[21] E. Baranoff, B. F. E. Curchod, F. Monti, F. Steimer, G. Accorsi, I. Tavernelli, U. Rothlisberger, R. Scopelliti, M. Gratzel, M. K. Nazeeruddin, *Inorg. Chem.*, 2012, **51**, 799-811.

[22] V. K. Rai, M. Nishiura, M. Takimoto, S. S. Zhao, Y. Liu, Z. M. Hou, *Inorg. Chem.*, 2012, **51**, 822-835.

[23] E. Orselli, G. S. Kottas, A. E. Konradsson, P. Coppo, R. Fröhlich, L. De Cola, A. Dijken, M. Büchel, H. Börner, *Inorg. Chem.*, 2007, **46**, 11082-11093.

[24] G.-J. Zhou, W.-Y. Wong, X. Yang *Chem. –Asian J.*, 2011, **6**, 1706-1727.

[25] W. Lee, T.-H. Kwon, J. Kwon, J. -Y. Kim, C. Lee, J.-I. Hong, *New J. Chem.*, 2011, **35**, 2557-2563.

[26] Y. J. Cho, K. R. Wee, H. J. Son, D. W. Cho, S. O. Kang, *Phys. Chem. Chem. Phys.*, 2014, **16**, 4510-4521.